Acta Cryst E CRYSTALLOGRAPHIC COMMUNICATIONS
ISSN 2056-9890

Crystal structure and Hirshfeld surface analysis of 2,2,2-trichloro-*N*,*N*-bis{[(1*RS*,4*SR*)-1,4-dihydro-1,4-epoxynaphthalen-1-yl]methyl}acetamide

Zeliha Atioğlu,[a] Mehmet Akkurt,[b] Gunay Z. Mammadova[c] and Ajaya Bhattarai[d]*

[a]Department of Aircraft Electrics and Electronics, School of Applied Sciences, Cappadocia University, Mustafapaşa, 50420 Ürgüp, Nevşehir, Turkey, [b]Department of Physics, Faculty of Sciences, Erciyes University, 38039 Kayseri, Turkey, [c]Organic Chemistry Department, Baku State University, Z. Khalilov str. 23, AZ 1148 Baku, Azerbaijan, and [d]Department of Chemistry, M.M.A.M.C (Tribhuvan University) Biratnagar, Nepal. *Correspondence e-mail: bkajaya@yahoo.com

Received 25 August 2021
Accepted 22 September 2021

Edited by A. V. Yatsenko, Moscow State University, Russia

Keywords: crystal structure; tetrahydrofuran rings; C—H···O hydrogen bonds; C—H···π interactions; Hirshfeld surface analysis; IMDAF reaction; Diels–Alder reaction.

CCDC reference: 2095762

Supporting information: this article has supporting information at journals.iucr.org/e

In the title compound, $C_{24}H_{18}Cl_3NO_3$, the tetrahydrofuran rings adopt envelope conformations. In the crystal, C—H···O hydrogen bonds connect molecules, generating layers parallel to the (001) plane. These layers are connected along the *c*-axis direction by C—H···π interactions. The packing is further stabilized by interlayer van der Waals and interhalogen interactions. The most important contributions to the surface contacts are from H···H (36.8%), Cl···H/H···Cl (26.6%), C···H/H···C (18.8%) and O···H/H···O (11.3%) interactions, as concluded from a Hirshfeld surface analysis.

1. Chemical context

In recent years, the IMDAF cycloaddition (the intramolecular furan Diels–Alder reaction) in combination with other known reactions in a tandem or sequential manner is pursued for the construction of several important bicyclic or polycyclic compounds, including natural ones (for some reviews on this topic, see: Zubkov *et al.*, 2005; Takao *et al.*, 2005; Juhl *et al.*, 2009; Padwa *et al.*, 2013; Parvatkar *et al.*, 2014; Krishna *et al.*, 2021). Cascade sequences comprising two or more successive [4 + 2] cycloaddition steps are a powerful and frequently used protocol in modern syntheses aimed at constructing cyclohexene derivatives thanks to their exceptional chemoselectivity, regioselectivity, diastereoselectivity, and capability to create more than four chiral centers in a single synthetic step (Criado *et al.*, 2010, 2013). It has been shown previously that the Diels–Alder reaction of bis-dienes with derivatives of maleic acid, esters of acetylene dicarboxylic acid and hexa-

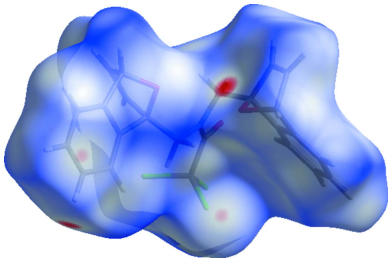

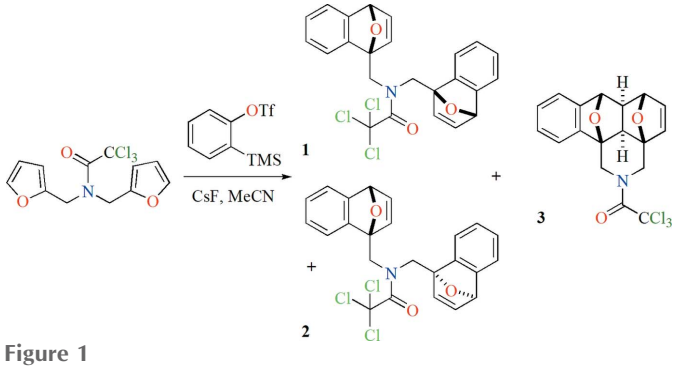

Figure 1
Synthesis scheme for 2,2,2-trichloro-*N*,*N*-bis[(1*R*,4*SR*)-1,4-epoxynaphthalen-1(4*H*)-ylmethyl]acetamide (**1**).

OPEN ACCESS

fluoro-2-butyne proceeds in all cases diastereo- and chemoselectively and leads, depending on the temperature, to annelated diepoxynaphthalenes of the 'domino' or 'pincer' type (Borisova *et al.*, 2018*a*,*b*; Grudova *et al.*, 2020; Kvyatkovskaya *et al.*, 2020, 2021). In order to expand the limits of the applicability of the IMDAF strategy, we tested in this study dehydrobenzene generated *in situ* in the role of dienophile. It was demonstrated that the products of the parallel [4 + 2] cycloaddition of two aryne moieties to both the furan fragments of the bis-diene system (Fig. 1, **1** and **2**) prevails over the adduct (**3**) of the IMDAF reaction (Fig. 1).

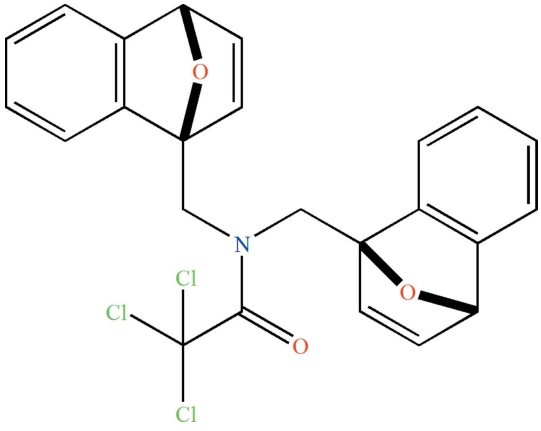

On the other hand, intermolecular non-covalent interactions organize the molecular aggregates, catalytic intermediates, *etc*., which play crucial roles for the functional properties of heterocyclic compounds (Gurbanov *et al.*, 2020*a*,*b*; Khalilov *et al.*, 2018*a*,*b*; Ma *et al.*, 2017*a*,*b*, 2020, 2021; Mahmudov *et al.*, 2020; Mizar *et al.*, 2012). Thus, attached –CCl_3 and C═O groups can participate in intermolecular interactions and affect the properties of **1**–**3**.

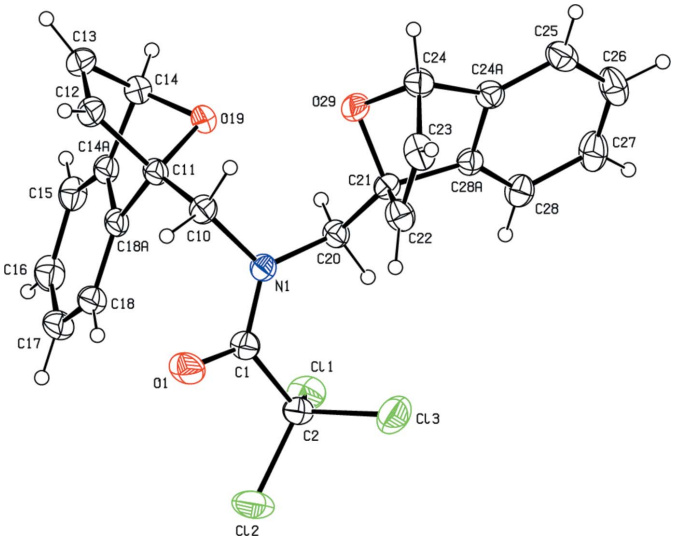

Figure 2
The molecule of the title compound **1** with atom-labeling scheme and displacement ellipsoids drawn at the 30% probability level. Hydrogen atoms are shown as spheres of arbitrary radius.

Table 1
Hydrogen-bond geometry (Å, °).

*Cg*8 is the centroid of the C24*A*/C25–C28/C28*A* aromatic ring.

D—H···*A*	*D*—H	H···*A*	*D*···*A*	*D*—H···*A*
C10—H10*A*···O29	0.97	2.35	3.074 (2)	131
C12—H12*A*···O1^{i}	0.93	2.66	3.494 (2)	150
C17—H17*A*···O1^{ii}	0.93	2.51	3.427 (3)	168
C20—H20*A*···O19	0.97	2.39	3.068 (2)	127
C27—H27*A*···O19^{iii}	0.93	2.51	3.438 (3)	175
C20—H20*B*···Cl1	0.97	2.55	3.1744 (18)	122
C20—H20*B*···Cl3	0.97	2.64	3.2921 (19)	125
C13—H13*A*···*Cg*8^{iv}	0.93	2.90	3.633 (2)	136

Symmetry codes: (i) $-x+\frac{3}{2}, y+\frac{1}{2}, -z+\frac{1}{2}$; (ii) $-x+\frac{3}{2}, y-\frac{1}{2}, -z+\frac{1}{2}$; (iii) $-x+\frac{1}{2}, y-\frac{1}{2}, -z+\frac{1}{2}$; (iv) $x-\frac{1}{2}, -y+\frac{1}{2}, z-\frac{1}{2}$.

2. Structural commentary

In the title compound (**1**, Fig. 2), the tetrahydrofuran rings (O19/C11–C14 and O29/C21–C24) adopt envelope conformations with the O atoms as the flaps. The molecular conformation is stabilized by intramolecular C10—H10*A*···O29 and C20—H20*A*···O19 hydrogen bonds and C20—H20*B*···Cl1 and C20—H20*B*···Cl3 interactions (Table 1).

3. Supramolecular features and Hirshfeld surface analysis

In the crystal, hydrogen bonds of the C—H···O type link the molecules, generating layers parallel to the (001) plane (Table 1; Figs. 3, 4, 5 and 6). These layers are connected by C—H···π interactions (C13—H13*A*···*Cg*8; Table 1), where *Cg*8 is

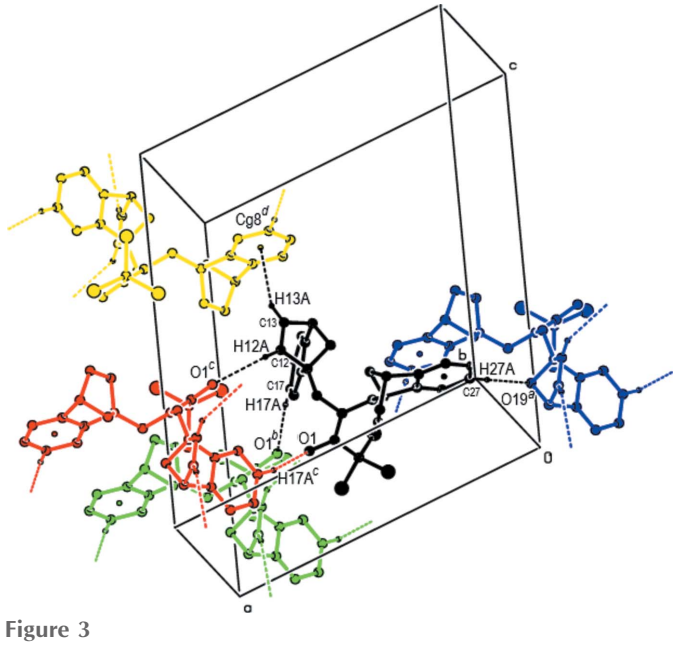

Figure 3
A general view of the intermolecular C—H···O hydrogen bonds and C—H···π interactions (depicted by dashed lines) in the unit cell of the title compound **1**. [Symmetry codes: (*a*) $\frac{1}{2}-x, -\frac{1}{2}+y, \frac{1}{2}-z$; (*b*) $\frac{3}{2}-x, -\frac{1}{2}+y, \frac{1}{2}-z$; (*c*) $\frac{3}{2}-x, \frac{1}{2}+y, \frac{1}{2}-z$; (*d*) $\frac{1}{2}+x, \frac{3}{2}-y, \frac{1}{2}+z$].

Table 2
Summary of short interatomic contacts (Å) in the title compound (**1**).

Contact	Distance	Symmetry operation
Cl1···H10*A*	3.10	$x, -1+y, z$
H20*A*···H25*A*	2.44	$\frac{1}{2}-x, -\frac{1}{2}+y, \frac{1}{2}-z$
H17*A*···O1	2.51	$\frac{3}{2}-x, -\frac{1}{2}+y, \frac{1}{2}-z$
H23*A*···Cl2	3.07	$1-x, 1-y, -z$
C28···H16*A*	2.96	$-\frac{1}{2}+x, \frac{1}{2}-y, -\frac{1}{2}+z$
H14*A*···C25	2.90	$-\frac{1}{2}+x, \frac{1}{2}-y, -\frac{1}{2}+z$
H15*A*···H14*A*	2.56	$1-x, 1-y, 1-z$

the centroid of the C24*A*/C25–C28/C28*A* aromatic ring. The intermolecular interactions in the crystal of the title compound (Table 2) were quantified using Hirshfeld surface analysis (Spackman & Jayatilaka, 2009) and the associated two-dimensional fingerprint plots (McKinnon *et al.*, 2007) were generated. The calculations and visualization were performed using *CrystalExplorer17* (Turner *et al.*, 2017). The

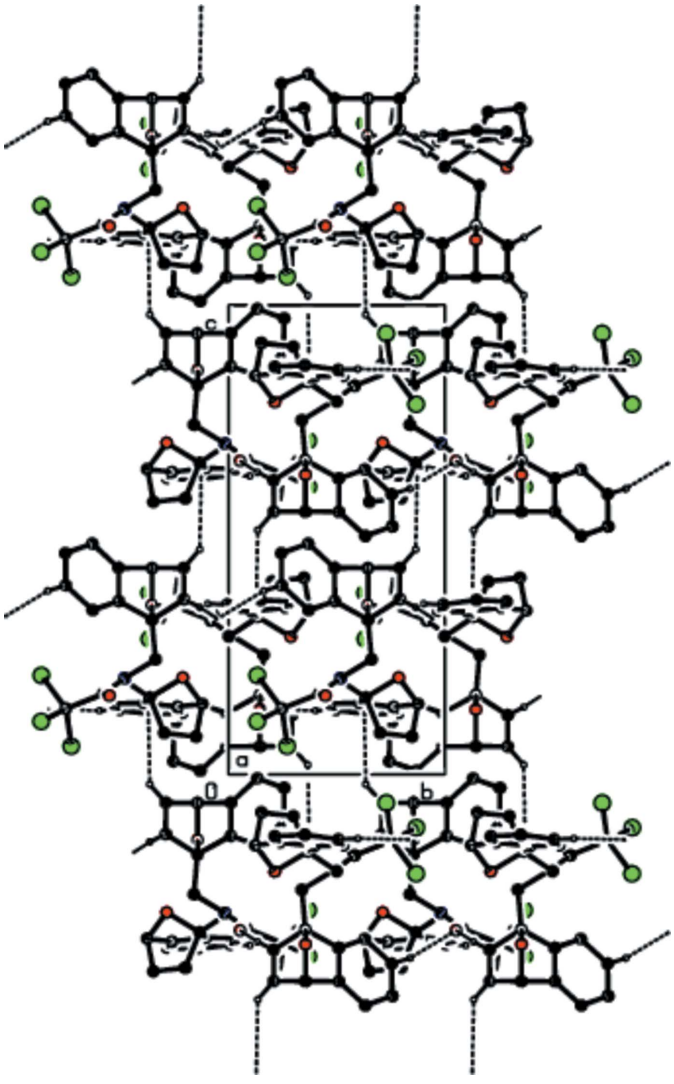

Figure 4
Packing viewed along the *a*-axis direction with the intermolecular C—H···O hydrogen bonds and C—H···π interactions depicted by dashed lines.

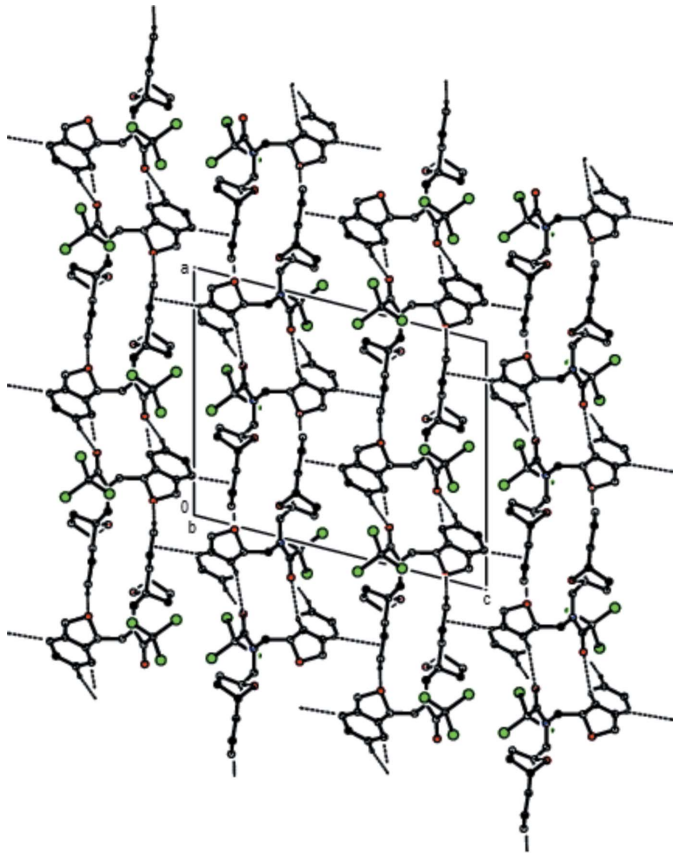

Figure 5
Packing viewed along the *b*-axis direction with the intermolecular C—H···O hydrogen bonds and C—H···π interactions depicted by dashed lines.

three-dimensional Hirshfeld surface mapped over d_{norm} in the range −0.1862 (red) to +1.4233 (blue) a.u. is shown in Fig. 7. The short and long contacts are indicated as red and blue spots, respectively, on the Hirshfeld surfaces, and contacts with distances approximately equal to the sum of the van der Waals radii are represented as white spots. The Cl···H and C—H···O interactions, which play a key role in the molecular packing, can be correlated with the bright-red patches near

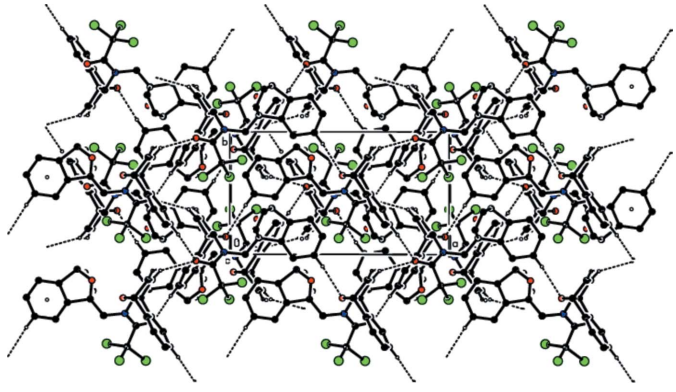

Figure 6
Packing viewed along the *c*-axis direction with the intermolecular C—H···O hydrogen bonds and C—H···π interactions depicted by dashed lines.

Table 3
Percentage contributions of interatomic contacts to the Hirshfeld surface for the title compound (**1**).

Contact	Percentage contribution
H···H	36.8
Cl···H/H···Cl	26.6
C···H/H···C	18.8
O···H/H···O	11.3
Cl···C/C···Cl	4.4
Cl···O/O···Cl	0.8
Cl···Cl	0.8
O···C/C···O	0.4
C···C	0.1

Cl1, Cl2, O1 and O19 and hydrogen atoms H14*A* and H16*A*, which highlight their functions as donors and/or acceptors. Fig. 8 shows the full two-dimensional fingerprint plot (Fig. 8*a*) and those delineated into the major contacts: H···H (36.8%, Fig. 8*b*) interactions are the major factor in the crystal packing together with Cl···H/H···Cl (26.6%, Fig. 8*c*), C···H/H···C (18.8%, Fig. 8*d*) and O···H/H···O (11.3%, Fig. 8*e*) interactions representing the next highest contributions. The percentage contributions of other weak interactions are listed in Table 3.

4. Database survey

A search of the Cambridge Structural Database (CSD version 5.40, update of September 2019; Groom *et al.*, 2016) for structures having the epoxyisoindole moiety gave ten hits that closely resemble the title compound, *viz.* 4,5-dibromo-2-[4-(trifluoromethyl)phenyl]hexahydro-3a,6-epoxyisoindol-1(4*H*)-one (CSD refcode IQOTOA; Mertsalov *et al.*, 2021*a*), 3-hydroxy-2-{[2-(4-methylbenzene-1-sulfonyl)-2,3,7,7a-tetrahydro-3a,6-epoxyisoindol-6(1*H*)-yl]methyl}-2,3-dihydro-1*H*-isoindol-1-one (OMUTAU; Mertsalov *et al.*, 2021*b*), 2-benzyl-4,5-dibromohexahydro-3a,6-epoxyisoindol-1(4*H*)-one (OMEMAX; Mertsalov *et al.*, 2021*c*), 4,5-dibromo-6-methyl-2-phenylhexahydro-3a,6-epoxyisoindol-1(4*H*)-one (IMUBIE; Mertsalov *et al.*, 2021*a*), (3a*R*,6*S*,7a*R*)-7a-chloro-2-[(4-nitrophenyl)sulfonyl]-1,2,3,6,7,7a-hexahydro-3a,6-epoxyisoindole (AGONUH; Temel *et al.*, 2013), (3a*R*,6*S*,7a*R*)-7a-chloro-6-methyl-2-[(4-nitrophenyl)sulfonyl]-1,2,3,6,7,7a-hexahydro-3a,6-epoxyisoindole (TIJMIK; Demircan *et al.*, 2013), 5-chloro-7-methyl-3-[(4-methyl-phenyl)sulfonyl]-10-oxa-3-aza-tricyclo[5.2.1.01,5]dec-8-ene (YAXCIL; Temel *et al.*, 2012), (3a*R*,6*S*,7a*R*)-7a-bromo-2-[(4-methylphenyl)sulfonyl]-1,2,3,6,-7,7a-hexahydro-3a,6-epoxyiso-indole (UPAQEI; Koşar *et al.*, 2011), (3a*R*,6*S*,7a*R*)-7a-bromo-2-methylsulfonyl-1,2,3,6,7,7-hexahydro-3a,6-epoxyisoindole (ERIVIL; Temel *et al.*, 2011) and *tert*-butyl 3a-chloroper-hydro-2,6a-epoxyoxireno(*e*)iso-indole-5-carboxylate (MIGTIG; Koşar *et al.*, 2007).

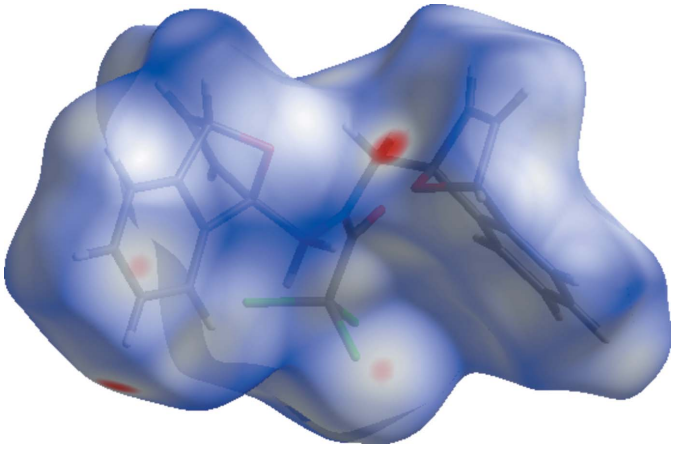

Figure 7
Hirshfeld surface of the title molecule **1** mapped with d_{norm}.

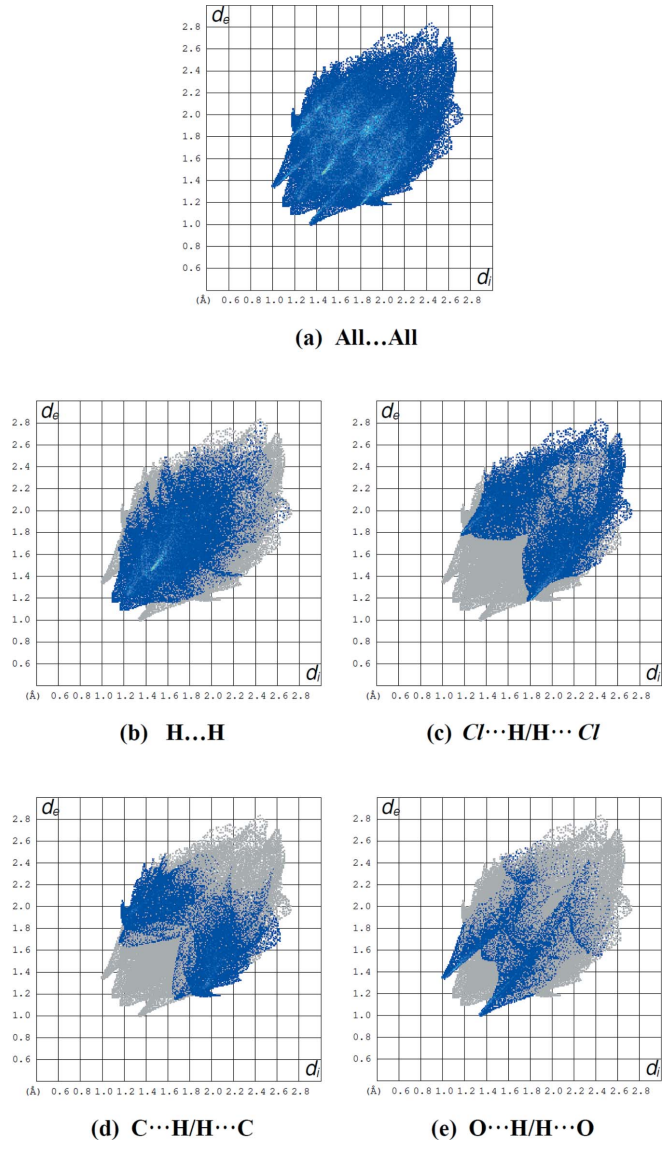

Figure 8
Fingerprint plots showing (*a*) all intermolecular interactions and resolved into (*b*) H···H, (*c*) Cl···H/H···Cl, (*d*) C···H/H···C and (*e*) O···H/H···O contacts.

In the crystal of IQOTOA, the asymmetric unit consists of two crystallographically independent molecules. In both molecules, the pyrrolidine and tetrahydrofuran rings adopt

envelope conformations. In the crystal, molecules are linked in pairs by C— H···O hydrogen bonds. These pairs form a tetrameric supramolecular motif, leading to molecular layers parallel to the (100) plane formed by C— H···π and C—Br···π interactions. OMUTAU also crystallizes with two independent molecules in the asymmetric unit. In the central ring systems of both molecules, the tetrahydrofuran rings adopt envelope conformations, the pyrrolidine rings adopt twisted-envelope conformations and the six-membered ring is in a boat conformation. In both molecules, the nine-membered groups attached to the central ring system are essentially planar. In the crystal, strong intermolecular O—H···O hydrogen bonds and weak intermolecular C—H···O contacts link the molecules, forming a three-dimensional network. In addition, weak π–π stacking interactions between the pyrrolidine rings are observed. OMEMAX again crystallizes with two molecules in the asymmetric unit of the unit cell. In both molecules, the tetrahydrofuran rings adopt envelope conformations with the O atoms as the flaps and the pyrrolidine rings also adopt envelope conformations. In the crystal, molecules are linked by weak C—H···O hydrogen bonds, forming sheets lying parallel to the (001) plane. These sheets are connected only by weak van der Waals interactions. In the crystal of IMUBIE, the molecules are linked into dimers by pairs of C—H···O hydrogen bonds, thus generating $R_2^2(18)$ rings. The crystal packing is dominated by H···H, Br···H, H···π and Br···π interactions. In the crystal structures of IQOTOA, OMUTAU, OMEMAX, AGONUH, TIJMIK, YAXCIL, UPAQEI and ERIVIL, the molecules are predominantly linked by C—H···O hydrogen bonds, giving various hydrogen-bonding pattern connectivities. In the crystal of AGONUH, the molecules are connected in zigzag chains running along the *b*-axis direction. In TIJMIK, two types of C—H···O hydrogen bonds are found, *viz.* $R^2_2(20)$ and $R^4_4(26)$ rings, with adjacent rings running parallel to the *ac* plane. Additionally, C—H···O hydrogen bonds form a $C(6)$ chain, linking the molecules in the *b*-axis direction. In the crystal of ERIVIL, the molecules are connected into $R_2^2(8)$ and $R_2^2(14)$ rings along the *b*-axis direction. In MIGTIG, the molecules are linked only by weak van der Waals interactions.

5. Synthesis and crystallization

CsF (1.7 g, 0.011 mol) was added to 2,2,2-trichloro-*N*,*N*-bis(-furan-2-ylmethyl)acetamide (0.0022 mol) dissolved in dry CH_3CN (20 mL). Then an equivalent of 2-(trimethylsilyl)phenyl trifluoromethanesulfonate (0.54 mL, 0.022 mol) was added to the solution under an argon atmosphere. The mixture was refluxed for 4 h (TLC control). After that, one more portion of 2-(trimethylsilyl)phenyl trifluoromethanesulfonate (0.27 mL, 0.011 mol) and CsF (1.7 g, 0.011 mol) was added to the mixture, repeating all procedures again. After the mixture was cooled, CsF was filtered off through a thin layer of SiO_2, and the resulting solution was concentrated under reduced pressure. The residue (brown oil) was separated using column chromatography on silica gel (a mixture EtOAc/hexane = 1/25 as eluent) to give compounds **1**–**3** in the ratio ~30/25/45. Single crystals of compound **1** was obtained by slow crystallization from a hexane/EtOAc mixture.

Compound **1**: white powder (0.29 g, 0.62 mmol, 28%); R_f 0.50 ('Sorbfil' plates for thin-layer chromatography, EtOAc/hexane, 1:4, Sorbfil); m.p. 431.7–433.4 K. ^{1}H NMR (600.2 MHz, $CDCl_3$) δ 7.19–7.24 (4H, m, H-Ar), 7.07 (1H, *dd*, *J* = 1.5 and *J* = 5.6 Hz, H-2′), 7.04 (2H, *br dd*, *J* = 2.0 and *J* = 5.0 Hz, H-3,3′), 6.95–6.99 (4H, *m*, H-Ar), 6.85 (1H, *d*, *J* = 5.6 Hz, H-2), 5.73 (1H, *d*, *J* = 1.5 Hz, H-4′), 5.71 (1H, *d*, *J* = 1.5 Hz, H-4), 5.11 (1H, *d*, *J* = 16.2 Hz, H-1′B), 4.87 (1H, *d*, *J* = 16.2 Hz, H-1B), 4.76 (1H, *d*, *J* = 15.1 Hz, H-1′A), 4.72 (1H, *br d*, *J* = 15.1 Hz, H-1A). ^{13}C NMR (150.9 MHz, $CDCl_3$) *d* 161.5, 150.2, 149.9, 148.7, 148.2, 145.2, 145.1, 143.3, 143.0, 125.5, 125.3, 125.2, 125.1, 120.5, 120.2, 120.0, 119.6, 94.1, 93.3, 92.1, 82.4, 82.2, 49.1, 45.6. IR νmax/cm^{-1} (tablet KBr): 2953, 2919, 1702, 1632, 1462, 1410, 1236. HRMS (ESI–TOF): calculated for $C_{24}H_{18}Cl_3NO_4$ $[M + H]^+$ 473.0352; found 473.0358.

Table 4
Experimental details.

Crystal data	
Chemical formula	$C_{24}H_{18}Cl_3NO_3$
M_r	474.74
Crystal system, space group	Monoclinic, $P2_1/n$
Temperature (K)	296
a, *b*, *c* (Å)	15.0134 (6), 8.1336 (3), 18.2841 (6)
β (°)	104.307 (2)
V (Å^3)	2163.48 (14)
Z	4
Radiation type	Mo $K\alpha$
μ (mm^{-1})	0.45
Crystal size (mm)	0.34 × 0.18 × 0.14
Data collection	
Diffractometer	Bruker Kappa APEXII area-detector diffractometer
Absorption correction	Multi-scan (*SADABS*; Bruker, 2013)
T_{min}, T_{max}	0.743, 0.940
No. of measured, independent and observed [$I > 2\sigma(I)$] reflections	17833, 4991, 3570
R_{int}	0.030
(sin $\theta/\lambda)_{max}$ (Å^{-1})	0.652
Refinement	
$R[F^2 > 2\sigma(F^2)]$, $wR(F^2)$, *S*	0.041, 0.118, 1.01
No. of reflections	4991
No. of parameters	280
H-atom treatment	H-atom parameters constrained
$\Delta\rho_{max}$, $\Delta\rho_{min}$ (e Å^{-3})	0.30, −0.36

Computer programs: *APEX2* and *SAINT* (Bruker, 2013), *SHELXT* (Sheldrick, 2015*a*), *SHELXL* (Sheldrick, 2015*b*), *ORTEP-3 for Windows* (Farrugia, 2012) and *PLATON* (Spek, 2020).

6. Refinement details

Crystal data, data collection and structure refinement details are summarized in Table 4. All C-bound H atoms were placed in calculated positions and refined using a riding model, with C—H = 0.93–0.98 Å, and with U_{iso}(H) = 1.2U_{eq}(C). Six reflections ($\bar{1}$01, 011, 101, 110, 002 and 200), which were obscured by the beam stop, and nine outliers (343, 253, $\bar{7}$,1,15, 3,6,11, 15,4,4, 072, 4,6,12, $\bar{4}$,3,22 and 13,6,2) were omitted during the final refinement cycle.

Acknowledgements

The authors' contributions are as follows. Conceptualization, MA and AB; synthesis, GZM; X-ray analysis, ZA and GZM; writing (review and editing of the manuscript), ZA, GZM and MA; supervision, MA and AB.

References

Borisova, K. K., Kvyatkovskaya, E. A., Nikitina, E. V., Aysin, R. R., Novikov, R. A. & Zubkov, F. I. (2018*a*). *J. Org. Chem.* **83**, 4840–4850.

Borisova, K. K., Nikitina, E. V., Novikov, R. A., Khrustalev, V. N., Dorovatovskii, P. V., Zubavichus, Y. V., Kuznetsov, M. L., Zaytsev, V. P., Varlamov, A. V. & Zubkov, F. I. (2018*b*). *Chem. Commun.* **54**, 2850–2853.

Bruker (2013). *APEX2*, *SAINT* and *SADABS*. Bruker AXS Inc., Madison, Wisconsin, USA.

Criado, A., Peña, D., Cobas, A. & Guitián, E. (2010). *Chem. Eur. J.* **16**, 9736–9740.

Criado, A., Vilas-Varela, M., Cobas, A., Pérez, D., Peña, D. & Guitián, E. (2013). *J. Org. Chem.* **78**, 12637–12649.

Demircan, A., Temel, E., Kandemir, M. K., Çolak, M. & Büyükgüngör, O. (2013). *Acta Cryst.* E**69**, o1628–o1629.

Farrugia, L. J. (2012). *J. Appl. Cryst.* **45**, 849–854.

Groom, C. R., Bruno, I. J., Lightfoot, M. P. & Ward, S. C. (2016). *Acta Cryst.* B**72**, 171–179.

Grudova, M. V., Gil, D. M., Khrustalev, V. N., Nikitina, E. V., Sinelshchikova, A. A., Grigoriev, M. S., Kletskov, A. V., Frontera, A. & Zubkov, F. I. (2020). *New J. Chem.* **44**, 20167–20180.

Gurbanov, A. V., Kuznetsov, M. L., Demukhamedova, S. D., Alieva, I. N., Godjaev, N. M., Zubkov, F. I., Mahmudov, K. T. & Pombeiro, A. J. L. (2020*a*). *CrystEngComm*, **22**, 628–633.

Gurbanov, A. V., Kuznetsov, M. L., Mahmudov, K. T., Pombeiro, A. J. L. & Resnati, G. (2020*b*). *Chem. Eur. J.* **26**, 14833–14837.

Juhl, M. & Tanner, D. (2009). *Chem. Soc. Rev.* **38**, 2983–2992.

Khalilov, A. N., Asgarova, A. R., Gurbanov, A. V., Maharramov, A. M., Nagiyev, F. N. & Brito, I. (2018*a*). *Z. Kristallogr. New Cryst. Struct.* **233**, 1019–1020.

Khalilov, A. N., Asgarova, A. R., Gurbanov, A. V., Nagiyev, F. N. & Brito, I. (2018*b*). *Z. Kristallogr. New Cryst. Struct.* **233**, 947–948.

Koşar, B., Demircan, A., Arslan, H. & Büyükgüngör, O. (2011). *Acta Cryst.* E**67**, o994–o995.

Koşar, B., Karaarslan, M., Demir, I. & Büyükgüngör, O. (2007). *Acta Cryst.* E**63**, o3323.

Krishna, G., Grudinin, D. G., Nikitina, E. V. & Zubkov, F. I. (2021). *Synthesis*, **53**, https://doi.org/10.1055/s-0040-1705983.

Kvyatkovskaya, E. A., Epifanova, P. P., Nikitina, E. V., Senin, A. A., Khrustalev, V. N., Polyanskii, K. B. & Zubkov, F. I. (2021). *New J. Chem.* **45**, 3400–3407.

Kvyatkovskaya, E. A., Nikitina, E. V., Khrustalev, V. N., Galmés, B., Zubkov, F. I. & Frontera, A. (2020). *Eur. J. Org. Chem.* pp. 156–161.

Ma, Z., Gurbanov, A. V., Maharramov, A. M., Guseinov, F. I., Kopylovich, M. N., Zubkov, F. I., Mahmudov, K. T. & Pombeiro, A. J. L. (2017*a*). *J. Mol. Catal. A Chem.* **426**, 526–533.

Ma, Z., Gurbanov, A. V., Sutradhar, M., Kopylovich, M. N., Mahmudov, K. T., Maharramov, A. M., Guseinov, F. I., Zubkov, F. I. & Pombeiro, A. J. L. (2017*b*). *Mol. Catal.* **428**, 17–23.

Ma, Z., Mahmudov, K. T., Aliyeva, V. A., Gurbanov, A. V., Guedes da Silva, M. F. C. & Pombeiro, A. J. L. (2021). *Coord. Chem. Rev.* **437**, 213859.

Ma, Z., Mahmudov, K. T., Aliyeva, V. A., Gurbanov, A. V. & Pombeiro, A. J. L. (2020). *Coord. Chem. Rev.* **423**, 213482.

Mahmudov, K. T., Gurbanov, A. V., Aliyeva, V. A., Resnati, G. & Pombeiro, A. J. L. (2020). *Coord. Chem. Rev.* **418**, 213381.

McKinnon, J. J., Jayatilaka, D. & Spackman, M. A. (2007). *Chem. Commun.* pp. 3814–3816.

Mertsalov, D. F., Alekseeva, K. A., Daria, M. S., Cheshigin, M. E., Çelikesir, S. T., Akkurt, M., Grigoriev, M. S. & Mlowe, S. (2021*a*). *Acta Cryst.* E**77**, 466–472.

Mertsalov, D. F., Nadirova, M. A., Sorokina, E. A., Vinokurova, M. A., Çelikesir, S. T., Akkurt, M., Kolesnik, I. A. & Bhattarai, A. (2021*b*). *Acta Cryst.* E**77**, 260–265.

Mertsalov, D. F., Zaytsev, V. P., Pokazeev, K. M., Grigoriev, M. S., Bachinsky, A. V., Çelikesir, S. T., Akkurt, M. & Mlowe, S. (2021*c*). *Acta Cryst.* E**77**, 255–259.

Mizar, A., Guedes da Silva, M. F. C., Kopylovich, M. N., Mukherjee, S., Mahmudov, K. T. & Pombeiro, A. J. L. (2012). *Eur. J. Inorg. Chem.* pp. 2305–2313.

Padwa, A. & Flick, A. C. (2013). *Adv. Heterocycl. Chem.* **110**, 1–41.

Parvatkar, P. T., Kadam, H. K. & Tilve, S. G. (2014). *Tetrahedron*, **70**, 2857–2888.

Sheldrick, G. M. (2015*a*). *Acta Cryst.* A**71**, 3–8.

Sheldrick, G. M. (2015*b*). *Acta Cryst.* C**71**, 3–8.

Spackman, M. A. & Jayatilaka, D. (2009). *CrystEngComm*, **11**, 19–32.

Spek, A. L. (2020). *Acta Cryst.* E**76**, 1–11.

Takao, K., Munakata, R. & Tadano, K. (2005). *Chem. Rev.* **105**, 4779–4807.

Temel, E., Demircan, A., Arslan, H. & Büyükgüngör, O. (2011). *Acta Cryst.* E**67**, o1304–o1305.

Temel, E., Demircan, A., Beyazova, G. & Büyükgüngör, O. (2012). *Acta Cryst.* E**68**, o1102–o1103.

Temel, E., Demircan, A., Kandemir, M. K., Çolak, M. & Büyükgüngör, O. (2013). *Acta Cryst.* E**69**, o1551–o1552.

Turner, M. J., McKinnon, J. J., Wolff, S. K., Grimwood, D. J., Spackman, P. R., Jayatilaka, D. & Spackman, M. A. (2017). *CrystalExplorer17*. The University of Western Australia.

Zubkov, F. I., Nikitina, E. V. & Varlamov, A. V. (2005). *Russ. Chem. Rev.* **74**, 639–669.

supporting information

Acta Cryst. (2021). E**77**, 1048-1053 [https://doi.org/10.1107/S2056989021009907]

Crystal structure and Hirshfeld surface analysis of 2,2,2-trichloro-*N*,*N*-bis-{[(1*RS*,4*SR*)-1,4-dihydro-1,4-epoxynaphthalen-1-yl]methyl}acetamide

Zeliha Atioğlu, Mehmet Akkurt, Gunay Z. Mammadova and Ajaya Bhattarai

Computing details

Data collection: *APEX2* (Bruker, 2013); cell refinement: *SAINT* (Bruker, 2013); data reduction: *SAINT* (Bruker, 2013); program(s) used to solve structure: SHELXT (Sheldrick, 2015a); program(s) used to refine structure: *SHELXL* (Sheldrick, 2015b); molecular graphics: *ORTEP-3 for Windows* (Farrugia, 2012); software used to prepare material for publication: *PLATON* (Spek, 2020).

2,2,2-Trichloro-*N*,*N*-bis{[(1*RS*,4*SR*)-1,4-dihydro-1,4-epoxynaphthalen-1-yl]methyl}acetamide

Crystal data

$C_{24}H_{18}Cl_3NO_3$
M_r = 474.74
Monoclinic, $P2_1/n$
a = 15.0134 (6) Å
b = 8.1336 (3) Å
c = 18.2841 (6) Å
β = 104.307 (2)°
V = 2163.48 (14) Å^3
Z = 4
$F(000)$ = 976
D_x = 1.458 Mg m^{-3}
Mo $K\alpha$ radiation, λ = 0.71073 Å
Cell parameters from 4831 reflections
θ = 2.8–26.7°
μ = 0.45 mm^{-1}
T = 296 K
Fragment, colourless
0.34 × 0.18 × 0.14 mm

Data collection

Bruker Kappa APEXII area-detector diffractometer
φ and ω scans
Absorption correction: multi-scan (SADABS; Bruker, 2013)
T_{min} = 0.743, T_{max} = 0.940
17833 measured reflections
4991 independent reflections
3570 reflections with $I > 2\sigma(I)$
R_{int} = 0.030
θ_{max} = 27.6°, θ_{min} = 3.2°
h = −19→19
k = −10→10
l = −23→23

Refinement

Refinement on F^2
Least-squares matrix: full
$R[F^2 > 2\sigma(F^2)]$ = 0.041
$wR(F^2)$ = 0.118
S = 1.01
4991 reflections
280 parameters
0 restraints
Hydrogen site location: inferred from neighbouring sites
H-atom parameters constrained
$w = 1/[\sigma^2(F_o^2) + (0.0576P)^2 + 0.6103P]$ where $P = (F_o^2 + 2F_c^2)/3$
$(\Delta/\sigma)_{max} < 0.001$
$\Delta\rho_{max}$ = 0.30 e Å^{-3}
$\Delta\rho_{min}$ = −0.36 e Å^{-3}

Special details

Geometry. All esds (except the esd in the dihedral angle between two l.s. planes) are estimated using the full covariance matrix. The cell esds are taken into account individually in the estimation of esds in distances, angles and torsion angles; correlations between esds in cell parameters are only used when they are defined by crystal symmetry. An approximate (isotropic) treatment of cell esds is used for estimating esds involving l.s. planes.

Fractional atomic coordinates and isotropic or equivalent isotropic displacement parameters (Å²)

	x	*y*	*z*	U_{iso}*/U_{eq}
C1	0.57432 (13)	0.4170 (2)	0.17193 (10)	0.0396 (4)
C2	0.53382 (14)	0.2461 (3)	0.14061 (12)	0.0450 (5)
C10	0.57234 (13)	0.6612 (2)	0.24521 (11)	0.0386 (4)
H10A	0.533570	0.757230	0.231289	0.046*
H10B	0.628106	0.679444	0.228600	0.046*
C11	0.59728 (12)	0.6449 (2)	0.32991 (11)	0.0353 (4)
C12	0.64935 (13)	0.7922 (2)	0.37350 (12)	0.0445 (5)
H12A	0.686507	0.866559	0.356181	0.053*
C13	0.63075 (14)	0.7916 (2)	0.44014 (12)	0.0473 (5)
H13A	0.651717	0.865687	0.479366	0.057*
C14	0.56784 (13)	0.6447 (2)	0.43983 (11)	0.0417 (4)
H14A	0.530748	0.647835	0.477024	0.050*
C14A	0.62536 (12)	0.4899 (2)	0.44023 (11)	0.0390 (4)
C15	0.65706 (14)	0.3678 (3)	0.49181 (12)	0.0466 (5)
H15A	0.643575	0.368000	0.538795	0.056*
C16	0.71008 (15)	0.2436 (3)	0.47154 (13)	0.0531 (5)
H16A	0.731376	0.158196	0.505157	0.064*
C17	0.73137 (15)	0.2450 (3)	0.40299 (13)	0.0521 (5)
H17A	0.767642	0.161342	0.391117	0.062*
C18	0.69959 (13)	0.3700 (2)	0.35035 (12)	0.0436 (4)
H18A	0.714646	0.371239	0.303977	0.052*
C18A	0.64551 (11)	0.4905 (2)	0.36943 (10)	0.0356 (4)
C20	0.42684 (12)	0.5001 (2)	0.20562 (10)	0.0359 (4)
H20A	0.422213	0.498360	0.257597	0.043*
H20B	0.404568	0.395232	0.183106	0.043*
C21	0.36523 (12)	0.6346 (2)	0.16411 (10)	0.0348 (4)
C22	0.37783 (13)	0.7010 (3)	0.08860 (11)	0.0440 (4)
H22A	0.405680	0.647375	0.055171	0.053*
C23	0.34135 (14)	0.8485 (3)	0.08083 (13)	0.0503 (5)
H23A	0.338084	0.920840	0.040843	0.060*
C24	0.30557 (14)	0.8769 (2)	0.15056 (12)	0.0467 (5)
H24A	0.296146	0.991967	0.162742	0.056*
C24A	0.22319 (13)	0.7630 (2)	0.14421 (10)	0.0396 (4)
C25	0.12998 (14)	0.7862 (3)	0.13138 (11)	0.0485 (5)
H25A	0.104624	0.891139	0.125152	0.058*
C26	0.07468 (15)	0.6477 (3)	0.12801 (12)	0.0556 (6)
H26A	0.011307	0.660262	0.118843	0.067*
C27	0.11209 (14)	0.4931 (3)	0.13797 (12)	0.0558 (6)
H27A	0.073843	0.402457	0.136186	0.067*

C28	0.20793 (13)	0.4696 (3)	0.15092 (11)	0.0448 (4)
H28A	0.233674	0.365028	0.157926	0.054*
C28A	0.26130 (12)	0.6058 (2)	0.15276 (9)	0.0350 (4)
N1	0.52425 (10)	0.51733 (18)	0.20508 (8)	0.0353 (3)
O1	0.65181 (10)	0.4475 (2)	0.16809 (9)	0.0594 (4)
O19	0.51694 (8)	0.64419 (16)	0.36140 (7)	0.0389 (3)
O29	0.37315 (9)	0.78716 (15)	0.20640 (7)	0.0431 (3)
Cl1	0.49921 (4)	0.13248 (6)	0.21124 (4)	0.05856 (17)
Cl2	0.61916 (5)	0.13144 (9)	0.11317 (5)	0.0795 (2)
Cl3	0.44055 (5)	0.27068 (8)	0.06047 (4)	0.0719 (2)

Atomic displacement parameters (Å²)

	U^{11}	U^{22}	U^{33}	U^{12}	U^{13}	U^{23}
C1	0.0400 (10)	0.0380 (10)	0.0425 (10)	−0.0010 (8)	0.0136 (8)	0.0011 (8)
C2	0.0436 (11)	0.0415 (10)	0.0510 (11)	0.0025 (8)	0.0138 (9)	−0.0063 (9)
C10	0.0366 (10)	0.0304 (9)	0.0486 (11)	−0.0056 (7)	0.0101 (8)	0.0000 (7)
C11	0.0276 (8)	0.0296 (9)	0.0489 (10)	−0.0020 (7)	0.0096 (7)	−0.0022 (7)
C12	0.0393 (11)	0.0305 (9)	0.0603 (13)	−0.0053 (8)	0.0060 (9)	−0.0042 (8)
C13	0.0465 (12)	0.0361 (10)	0.0552 (12)	−0.0006 (9)	0.0051 (9)	−0.0105 (9)
C14	0.0358 (10)	0.0437 (11)	0.0449 (10)	−0.0001 (8)	0.0088 (8)	−0.0059 (8)
C14A	0.0309 (9)	0.0356 (10)	0.0485 (10)	−0.0048 (7)	0.0062 (7)	−0.0043 (8)
C15	0.0417 (11)	0.0463 (11)	0.0489 (11)	−0.0066 (9)	0.0056 (9)	0.0023 (9)
C16	0.0491 (12)	0.0401 (11)	0.0632 (14)	0.0007 (9)	0.0006 (10)	0.0081 (10)
C17	0.0450 (12)	0.0366 (10)	0.0707 (14)	0.0091 (9)	0.0067 (10)	−0.0039 (10)
C18	0.0382 (10)	0.0389 (10)	0.0536 (12)	0.0009 (8)	0.0109 (8)	−0.0047 (8)
C18A	0.0266 (8)	0.0312 (9)	0.0473 (10)	−0.0040 (7)	0.0060 (7)	−0.0008 (7)
C20	0.0323 (9)	0.0329 (9)	0.0431 (10)	−0.0024 (7)	0.0102 (7)	0.0010 (7)
C21	0.0346 (9)	0.0309 (9)	0.0383 (9)	−0.0023 (7)	0.0082 (7)	−0.0031 (7)
C22	0.0381 (10)	0.0508 (12)	0.0455 (11)	−0.0010 (9)	0.0150 (8)	0.0056 (9)
C23	0.0445 (11)	0.0458 (12)	0.0601 (13)	−0.0024 (9)	0.0118 (9)	0.0166 (10)
C24	0.0445 (11)	0.0323 (10)	0.0595 (13)	0.0040 (8)	0.0058 (9)	−0.0005 (9)
C24A	0.0406 (10)	0.0413 (10)	0.0370 (9)	0.0020 (8)	0.0098 (7)	−0.0010 (8)
C25	0.0463 (12)	0.0594 (13)	0.0416 (10)	0.0136 (10)	0.0142 (9)	0.0030 (9)
C26	0.0345 (10)	0.0849 (18)	0.0496 (12)	0.0021 (11)	0.0149 (9)	0.0111 (11)
C27	0.0412 (11)	0.0735 (16)	0.0533 (12)	−0.0185 (11)	0.0125 (9)	0.0043 (11)
C28	0.0438 (11)	0.0458 (11)	0.0446 (10)	−0.0064 (9)	0.0106 (8)	0.0017 (9)
C28A	0.0346 (9)	0.0410 (10)	0.0302 (8)	−0.0022 (7)	0.0093 (7)	−0.0020 (7)
N1	0.0325 (8)	0.0314 (8)	0.0418 (8)	−0.0030 (6)	0.0086 (6)	−0.0015 (6)
O1	0.0475 (9)	0.0566 (9)	0.0848 (11)	−0.0086 (7)	0.0368 (8)	−0.0112 (8)
O19	0.0279 (6)	0.0422 (7)	0.0460 (7)	0.0007 (5)	0.0081 (5)	−0.0044 (6)
O29	0.0429 (8)	0.0311 (7)	0.0497 (8)	0.0011 (6)	0.0011 (6)	−0.0067 (6)
Cl1	0.0690 (4)	0.0354 (3)	0.0743 (4)	−0.0035 (2)	0.0234 (3)	0.0056 (2)
Cl2	0.0716 (4)	0.0686 (4)	0.1080 (6)	0.0077 (3)	0.0409 (4)	−0.0319 (4)
Cl3	0.0757 (4)	0.0686 (4)	0.0586 (4)	−0.0006 (3)	−0.0076 (3)	−0.0129 (3)

Geometric parameters (Å, º)

C1—O1	1.209 (2)	C17—H17A	0.9300
C1—N1	1.351 (2)	C18—C18A	1.372 (3)
C1—C2	1.568 (3)	C18—H18A	0.9300
C2—Cl2	1.755 (2)	C20—N1	1.472 (2)
C2—Cl1	1.767 (2)	C20—C21	1.510 (2)
C2—Cl3	1.770 (2)	C20—H20A	0.9700
C10—N1	1.472 (2)	C20—H20B	0.9700
C10—C11	1.506 (3)	C21—O29	1.451 (2)
C10—H10A	0.9700	C21—C22	1.537 (3)
C10—H10B	0.9700	C21—C28A	1.540 (2)
C11—O19	1.459 (2)	C22—C23	1.312 (3)
C11—C18A	1.538 (2)	C22—H22A	0.9300
C11—C12	1.540 (2)	C23—C24	1.519 (3)
C12—C13	1.316 (3)	C23—H23A	0.9300
C12—H12A	0.9300	C24—O29	1.447 (2)
C13—C14	1.522 (3)	C24—C24A	1.527 (3)
C13—H13A	0.9300	C24—H24A	0.9800
C14—O19	1.449 (2)	C24A—C25	1.374 (3)
C14—C14A	1.526 (3)	C24A—C28A	1.394 (3)
C14—H14A	0.9800	C25—C26	1.392 (3)
C14A—C15	1.371 (3)	C25—H25A	0.9300
C14A—C18A	1.400 (3)	C26—C27	1.371 (3)
C15—C16	1.392 (3)	C26—H26A	0.9300
C15—H15A	0.9300	C27—C28	1.412 (3)
C16—C17	1.368 (3)	C27—H27A	0.9300
C16—H16A	0.9300	C28—C28A	1.362 (3)
C17—C18	1.400 (3)	C28—H28A	0.9300
O1—C1—N1	123.52 (18)	C18—C18A—C11	134.72 (18)
O1—C1—C2	116.95 (17)	C14A—C18A—C11	104.65 (15)
N1—C1—C2	119.42 (16)	N1—C20—C21	114.45 (14)
C1—C2—Cl2	109.31 (13)	N1—C20—H20A	108.6
C1—C2—Cl1	110.74 (13)	C21—C20—H20A	108.6
Cl2—C2—Cl1	107.36 (11)	N1—C20—H20B	108.6
C1—C2—Cl3	110.99 (14)	C21—C20—H20B	108.6
Cl2—C2—Cl3	107.91 (11)	H20A—C20—H20B	107.6
Cl1—C2—Cl3	110.41 (11)	O29—C21—C20	113.09 (14)
N1—C10—C11	114.17 (14)	O29—C21—C22	99.57 (14)
N1—C10—H10A	108.7	C20—C21—C22	120.64 (16)
C11—C10—H10A	108.7	O29—C21—C28A	98.57 (13)
N1—C10—H10B	108.7	C20—C21—C28A	115.56 (14)
C11—C10—H10B	108.7	C22—C21—C28A	106.13 (14)
H10A—C10—H10B	107.6	C23—C22—C21	106.13 (18)
O19—C11—C10	112.73 (14)	C23—C22—H22A	126.9
O19—C11—C18A	98.64 (13)	C21—C22—H22A	126.9
C10—C11—C18A	121.53 (15)	C22—C23—C24	105.84 (18)

O19—C11—C12	99.35 (14)	C22—C23—H23A	127.1
C10—C11—C12	115.42 (15)	C24—C23—H23A	127.1
C18A—C11—C12	105.78 (15)	O29—C24—C23	100.59 (15)
C13—C12—C11	106.25 (17)	O29—C24—C24A	99.27 (15)
C13—C12—H12A	126.9	C23—C24—C24A	106.97 (16)
C11—C12—H12A	126.9	O29—C24—H24A	115.9
C12—C13—C14	105.83 (17)	C23—C24—H24A	115.9
C12—C13—H13A	127.1	C24A—C24—H24A	115.9
C14—C13—H13A	127.1	C25—C24A—C28A	121.17 (18)
O19—C14—C13	100.44 (15)	C25—C24A—C24	134.57 (19)
O19—C14—C14A	99.30 (14)	C28A—C24A—C24	104.24 (16)
C13—C14—C14A	107.32 (15)	C24A—C25—C26	117.9 (2)
O19—C14—H14A	115.8	C24A—C25—H25A	121.0
C13—C14—H14A	115.8	C26—C25—H25A	121.0
C14A—C14—H14A	115.8	C27—C26—C25	121.08 (19)
C15—C14A—C18A	121.38 (18)	C27—C26—H26A	119.5
C15—C14A—C14	134.49 (18)	C25—C26—H26A	119.5
C18A—C14A—C14	104.12 (16)	C26—C27—C28	120.9 (2)
C14A—C15—C16	117.8 (2)	C26—C27—H27A	119.6
C14A—C15—H15A	121.1	C28—C27—H27A	119.6
C16—C15—H15A	121.1	C28A—C28—C27	117.6 (2)
C17—C16—C15	121.1 (2)	C28A—C28—H28A	121.2
C17—C16—H16A	119.5	C27—C28—H28A	121.2
C15—C16—H16A	119.5	C28—C28A—C24A	121.36 (17)
C16—C17—C18	121.3 (2)	C28—C28A—C21	134.20 (17)
C16—C17—H17A	119.4	C24A—C28A—C21	104.43 (15)
C18—C17—H17A	119.4	C1—N1—C20	127.57 (15)
C18A—C18—C17	117.81 (19)	C1—N1—C10	116.44 (15)
C18A—C18—H18A	121.1	C20—N1—C10	115.99 (14)
C17—C18—H18A	121.1	C14—O19—C11	96.05 (13)
C18—C18A—C14A	120.62 (17)	C24—O29—C21	96.01 (13)

O1—C1—C2—Cl2	4.6 (2)	C21—C22—C23—C24	0.0 (2)
N1—C1—C2—Cl2	−171.75 (15)	C22—C23—C24—O29	33.4 (2)
O1—C1—C2—Cl1	122.72 (17)	C22—C23—C24—C24A	−69.8 (2)
N1—C1—C2—Cl1	−53.7 (2)	O29—C24—C24A—C25	146.2 (2)
O1—C1—C2—Cl3	−114.28 (18)	C23—C24—C24A—C25	−109.7 (2)
N1—C1—C2—Cl3	69.3 (2)	O29—C24—C24A—C28A	−35.51 (18)
N1—C10—C11—O19	−67.92 (19)	C23—C24—C24A—C28A	68.64 (19)
N1—C10—C11—C18A	48.7 (2)	C28A—C24A—C25—C26	0.7 (3)
N1—C10—C11—C12	178.87 (15)	C24—C24A—C25—C26	178.8 (2)
O19—C11—C12—C13	32.80 (19)	C24A—C25—C26—C27	0.7 (3)
C10—C11—C12—C13	153.59 (17)	C25—C26—C27—C28	−0.9 (3)
C18A—C11—C12—C13	−69.00 (19)	C26—C27—C28—C28A	−0.3 (3)
C11—C12—C13—C14	0.4 (2)	C27—C28—C28A—C24A	1.7 (3)
C12—C13—C14—O19	−33.89 (19)	C27—C28—C28A—C21	−179.31 (18)
C12—C13—C14—C14A	69.4 (2)	C25—C24A—C28A—C28	−1.9 (3)
O19—C14—C14A—C15	−144.6 (2)	C24—C24A—C28A—C28	179.46 (17)

C13—C14—C14A—C15	111.3 (2)	C25—C24A—C28A—C21	178.80 (17)
O19—C14—C14A—C18A	36.13 (17)	C24—C24A—C28A—C21	0.19 (18)
C13—C14—C14A—C18A	−67.96 (18)	O29—C21—C28A—C28	−144.1 (2)
C18A—C14A—C15—C16	−0.1 (3)	C20—C21—C28A—C28	−23.4 (3)
C14—C14A—C15—C16	−179.27 (19)	C22—C21—C28A—C28	113.2 (2)
C14A—C15—C16—C17	1.3 (3)	O29—C21—C28A—C24A	35.00 (16)
C15—C16—C17—C18	−0.9 (3)	C20—C21—C28A—C24A	155.77 (15)
C16—C17—C18—C18A	−0.6 (3)	C22—C21—C28A—C24A	−67.64 (17)
C17—C18—C18A—C14A	1.8 (3)	O1—C1—N1—C20	172.92 (18)
C17—C18—C18A—C11	−179.78 (19)	C2—C1—N1—C20	−10.9 (3)
C15—C14A—C18A—C18	−1.5 (3)	O1—C1—N1—C10	−6.9 (3)
C14—C14A—C18A—C18	177.93 (16)	C2—C1—N1—C10	169.28 (16)
C15—C14A—C18A—C11	179.68 (16)	C21—C20—N1—C1	−114.5 (2)
C14—C14A—C18A—C11	−0.92 (17)	C21—C20—N1—C10	65.2 (2)
O19—C11—C18A—C18	147.2 (2)	C11—C10—N1—C1	−104.29 (19)
C10—C11—C18A—C18	23.7 (3)	C11—C10—N1—C20	75.91 (19)
C12—C11—C18A—C18	−110.5 (2)	C13—C14—O19—C11	52.63 (15)
O19—C11—C18A—C14A	−34.20 (16)	C14A—C14—O19—C11	−57.06 (15)
C10—C11—C18A—C14A	−157.68 (16)	C10—C11—O19—C14	−174.45 (14)
C12—C11—C18A—C14A	68.14 (18)	C18A—C11—O19—C14	55.97 (14)
N1—C20—C21—O29	−76.82 (19)	C12—C11—O19—C14	−51.72 (15)
N1—C20—C21—C22	40.7 (2)	C23—C24—O29—C21	−52.34 (16)
N1—C20—C21—C28A	170.63 (14)	C24A—C24—O29—C21	57.01 (16)
O29—C21—C22—C23	−33.12 (19)	C20—C21—O29—C24	−178.99 (15)
C20—C21—C22—C23	−157.33 (17)	C22—C21—O29—C24	51.68 (16)
C28A—C21—C22—C23	68.77 (19)	C28A—C21—O29—C24	−56.40 (15)

Hydrogen-bond geometry (Å, º)

*Cg*8 is the centroid of the C24*A*/C25–C28/C28*A* aromatic ring.

D—H···*A*	*D*—H	H···*A*	*D*···*A*	*D*—H···*A*
C10—H10*A*···O29	0.97	2.35	3.074 (2)	131
C12—H12*A*···O1^{i}	0.93	2.66	3.494 (2)	150
C17—H17*A*···O1^{ii}	0.93	2.51	3.427 (3)	168
C20—H20*A*···O19	0.97	2.39	3.068 (2)	127
C27—H27*A*···O19^{iii}	0.93	2.51	3.438 (3)	175
C20—H20*B*···Cl1	0.97	2.55	3.1744 (18)	122
C20—H20*B*···Cl3	0.97	2.64	3.2921 (19)	125
C13—H13*A*···*Cg*8^{iv}	0.93	2.90	3.633 (2)	136

Symmetry codes: (i) −*x*+3/2, *y*+1/2, −*z*+1/2; (ii) −*x*+3/2, *y*−1/2, −*z*+1/2; (iii) −*x*+1/2, *y*−1/2, −*z*+1/2; (iv) *x*−1/2, −*y*+1/2, *z*−1/2.